PHILOSOPHICAL TRANSACTIONS OF THE ROYAL SOCIETY A MATHEMATICAL, PHYSICAL & ENGINEERING SCIENCES

Nanocrystals and Nano-Optics

L. E. Brus and J. K. Trautman

Phil. Trans. R. Soc. Lond. A 1995 **353**, 313-321
doi: 10.1098/rsta.1995.0102

Nanocrystals and nano-optics

By L. E. Brus and J. K. Trautman
AT&T Bell Laboratories, Murray Hill, NJ 07974, USA

Three dimensional electronic quantum confinement in semiconductor nanocrystals, and near-field optical spectroscopy of single molecules, are briefly discussed as examples of new science and technology at the nanometer scale.

1. Introduction

In this short article we describe two areas of science and technology of interest to the present NATO Advanced Research Workshop on 'The Ultimate Limits of Fabrication and Measurement'. Both areas explore phenomena on length scales less than the natural length scale of the corresponding bulk systems. In nanocrystals, the bulk length scale is the intrinsic delocalization length of electrons and holes in macroscopic semiconductors. In optics, the length scale is the optical wavelength.

In the area of semiconductor nanocrystals, the size-dependent development of band structure and bulk-like optical properties is explored in nanocrystals of dimension 1–10 nm. In this regime the electron and hole dynamics are quantum confined in three dimensions. Such nanocrystals are often labelled quantum dots. Two examples are given: direct gap CdSe and indirect gap Si. We will see that, heuristically, the principal effect of confinement in CdSe is spectroscopic, while the principal effect of confinement in Si is kinetic.

In near field scanning optical microscopy (NSOM), the nano-optical technique discussed here, light is confined to about 1/10 of an optical wavelength, enabling one to measure optical properties on a length scale of 10–100 nm. In particular, we have used the sensitivity afforded by NSOM to obtain the luminescence spectra of single molecules and nanocrystals, at room temperature. This permits direct observation of spectral changes caused by variations in the local environment of molecules in amorphous materials, and, more generally, the spectral differences caused by the existence of spatially varying structure in real materials.

2. Semiconductor nanocrystals

(*a*) *Spectroscopic and kinetic size regimes*

Figure 1 shows a schematic outline of different size regimes in the development of bulk properties with increasing size. In spectroscopic properties, one can recognize three size regimes: molecular, quantum dot (alternately, nanocrystal or quantum crystallite), and polariton (Brus 1986). In very small clusters of 10–50 atoms, the diamond lattice is not stable with respect to isomerization into molecular structures which eliminate broken surface bonds. The bulk unit cell is not present in this molecular regime. In the quantum dot regime (1–10 nm), the physical structure is now that

Phil. Trans. R. Soc. Lond. A (1995) **353**, 313–321
Printed in Great Britain

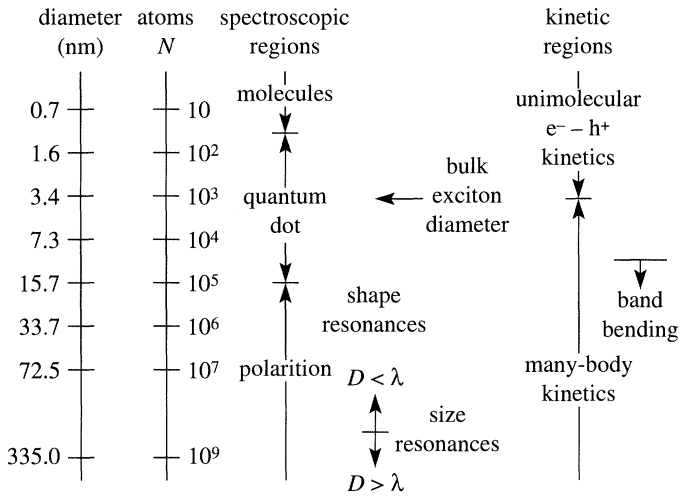

Figure 1. Schematic of size regimes for semiconductor nanocrystals.

of an excised fragment of the bulk lattice. However, the electronic properties show strong three dimensional quantum confinement; the excited states are discrete, and the band gap is shifted to higher energy. Strong confinement persists for nanocrystal diameters less than the Bohr bulk exciton diameter. In the polariton regime, as the bulk band gap develops with increasing size, the interaction with the electromagnetic field becomes strong and must be included in zero order. Local field effects develop, and the crystallites show shape and size resonances as described by Mie scattering theory.

The kinetic changes are equally interesting. In the molecular and quantum dot regimes, the kinetics are unimolecular: essentially those of a single electron–hole pair interacting with each other and the lattice. Confinement within one nanocrystal prevents the two carriers from separating, and from interacting with other pairs in other crystallites. At typical intrinsic doping levels, there is less than one dopant per nanocrystal, and therefore there is no band bending at the surface. Surface states, if they exist resonant with or inside the nanocrystal band gap, dominate the recombination kinetics. As such a crystallite grows, the kinetics evolves from molecule-like to solid-state-like. Band bending develops, and the excitation probability of multiple pairs inside one crystallite scales with volume. As confinement energies become less than kT, the carriers are independently mobile over the entire crystallite, and recombine by many-body scattering kinetics.

(*b*) *Direct gap* CdSe

CdSe is quite similar to InP and GaAs in band structure, and typifies quantum confinement for the II–VI and III–V direct gap materials. CdSe samples of very high quality, in terms of crystallinity and monodispersity in size, have been made by organometallic liquid phase synthesis (Steigerwald *et al.* 1988; Bawendi *et al.* 1989; Murray *et al.* 1993). For this reason, CdSe has become the prototype for three dimensional quantum confinement in semiconductors. The room temperature optical spectra show that discrete structure develops as size decreases from about 10 nm to 1.5 nm. In this same range the band gap increases from the bulk value 1.7 eV, to 3.2 eV in the smallest nanocrystal.

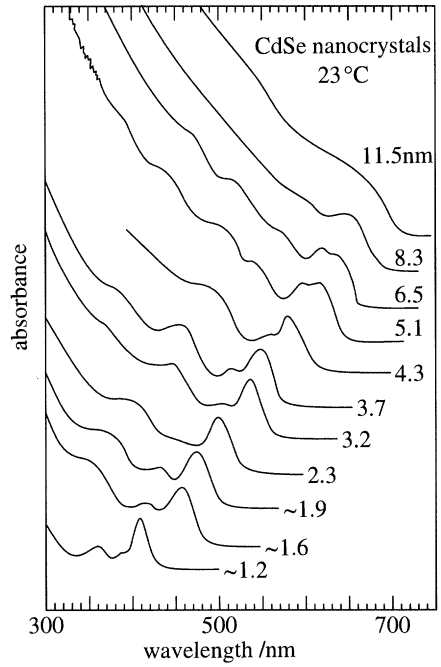

Figure 2. CdSe optical spectra adapted from Murray *et al.* (1993).

It is possible to understand all the strong transitions in these low resolution spectra in a model in which the electron and hole are confined inside a spherical nanocrystal, with the surface simply taken as a mathematical confining barrier (Chestnoy *et al.* 1986; Xia 1989; Ekimov *et al.* 1993; Norris *et al.* 1994). In II–VI and III–V semiconductors, the electron is s-like and the hole p-like within the unit cell. In CdSe, the lowest electron level is the totally symmetric combination of s orbitals, principally on Cd atoms, multiplied by an envelope function that has nodes on the crystallite surface. Because of this s nature, and the fact the electron effective mass is only $0.12m_e$, the electron energy levels (i.e. molecular orbitals) are sparse in energy, as shown in figure 3. However, the hole molecular orbitals are more dense in energy, because of the three fold spatial degeneracy of the p orbital, and because the hole is heavier than the electron. Most of the strong transitions in figure 2 involve transitions from various hole levels to the lowest ^{1}s electron level. Thus the complexity in the optical spectrum is in fact a measure of complexity in the three dimensionally quantized valence band.

The band gap ^{1}s–^{1}s internal transition has been studied in detail by various optical methods: low temperature hole burning, femtosecond coherent pump-and-probe, and size selective photoluminescence excitation (Bawendi *et al.* 1990, 1992; Schoenlein *et al.* 1993). The transition shows *LO* phonon structure, and the zero phonon line (ZPL) has a temperature dependent width due to coupling with the acoustical breathing mode of the nanocrystal. Additionally, the ZPL has a lineshape at low temperature that reflects fast dynamical relaxation of the optically created ^{1}s hole into surface states, essentially resonant in energy with the ^{1}s internal molecular orbital. These surface states are thought to be lone pair electrons on surface Se atoms. The luminescence decay kinetics shows temperature dependent equilibration, apparently among the various possible hole states.

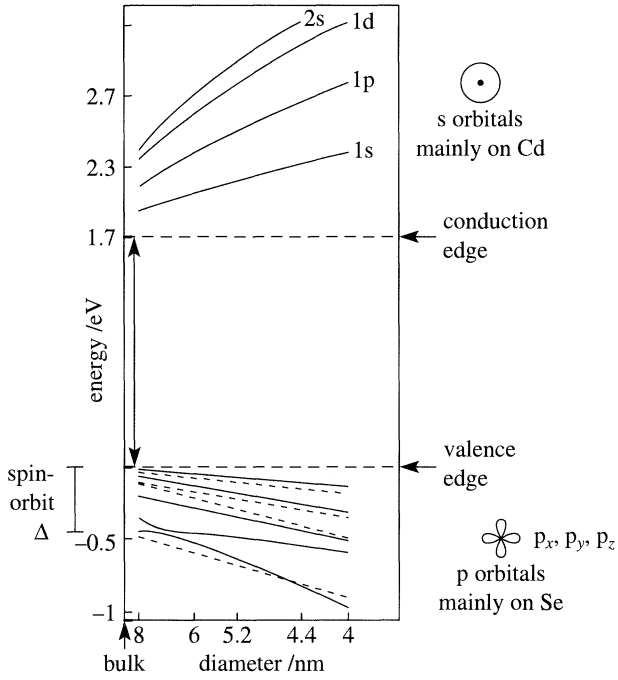

Figure 3. CdSe confined molecular orbitals, adpated from Ekimov *et al.* (1993).

(*c*) *Indirect gap silicon*

In direct gap CdSe the band gap optical transition is allowed under electron dipole selection rules for all sizes. The oscillator strength for the lowest ^{1}s–^{1}s transition is near one, corresponding to nanosecond radiative emission lifetimes. Silicon is indirect gap, and thus luminescence is electron dipole forbidden in the bulk crystal where the electron momentum k is a good quantum number. A new aspect of confinement physics in silicon is the prediction that luminescence will become weakly dipole allowed without phonon participation in nanocrystals (Takagahara & Takeda 1992; Proot *et al.* 1992). k is not a good quantum number in nanocrystals as a Fourier superposition in k is required to spatially localized a carrier inside a nanocrystal.

This idea of enhanced oscillator strength, essentially a partial direct-gap-like character in nanocrystals, has been proposed to explain the room temperature luminescence of porous silicon films (Canham 1990; Lehmann & Gosele 1991). These films are made of nm size wires and crystallites, in an irregular sponge network. These films have band gaps larger than bulk silicon, and shows near infrared (600–800 nm) luminescence at room temperature, above the bulk Si band gap at 1.1 eV. Si shell crystallites, with a 0.5–0.7 nm surface oxide and an interior of diamond lattice crystalline silicon, also show efficient luminescence with similar decay lifetimes in this same spectral region (Littau *et al.* 1993; Wilson *et al.* 1993; Schuppler *et al.* 1994). Quantum yields are near 5% at room temperature, increasing to near 50% at low temperature. Figure 4 shows a luminescence excitation spectrum of small crystallites, near 1.5 nm in Si core size, which emit at 2.0 eV (630 nm).

In contrast to CdSe, there is no resolved discrete structure; the optical spectrum appears to be that of an indirect gap material with a band gap near 2.0 eV. An analysis of the temperature dependent unimolecular decay dynamics shows that the

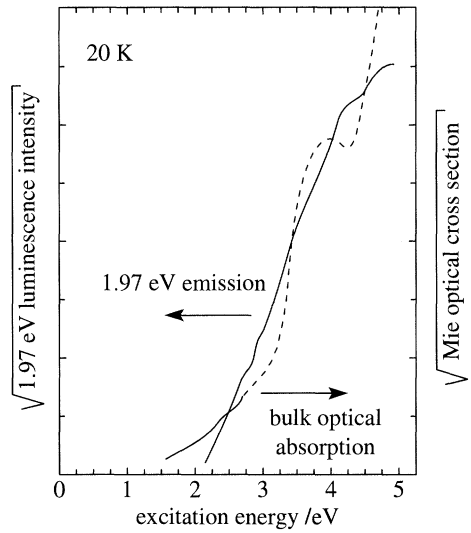

Figure 4. Luminescence excitation spectra of Si nanocrystals, adapted from Wilson *et al.* (1993).

radiative lifetime remains quite long, about 5×10^{-4} s, despite the high quantum yield of luminescence. Actually, in the Si shell nanocrystals, the radiative lifetime is somewhat longer than the 5×10^{-5} s radiative lifetime of the hydrogenic exciton in bulk Si at low temperature. Thus the reason that luminescence increases in Si nanocrystals, and apparently also in porous silicon, is not an increase in oscillator strength, but instead a decrease in radiationless transitions that compete with radiative recombination in the bulk (Brus 1994). At room temperature in bulk Si, electron hole pairs are not bound with respect to kT, and thus carriers move independently in the crystal. Under moderate optical excitation densities, three-body Auger non-radiative recombination,

$$(e^- + h^+) + e^- \rightarrow e^- + 1.1\ \text{eV}\ \ \text{kinetic energy}$$

dominates the kinetics. The effect of three-dimensional quantum confinement in isolated nanocrystals is two fold: (*a*) $e^- + h^+$ are superimposed on each other at 293 K by confinement in one crystallite, and (*b*) the Auger process is shut off, as pairs in separate nanocrystals do not interact. If the surface passivation is good and does not introduce new non-radiative routes, then a pair combines radiatively on a slow, near bulk-like time scale. In essence, the conversion from solid-state-kinetics to molecular kinetics causes the increase in luminescence (Brus *et al.* 1995).

3. Near field scanning optical microscopy

(*a*) *Single molecule and nanocrystal emission spectra*

In the optical studies of nanocrystals, a serious problem is the inhomogeneous broadening of the spectra due to the size, shape, and structural distributions present in even the best samples. These distributions cause the spectral structure intrinsic to individual nanocrystals to be averaged out in the spectra obtained by traditional methods. It would be an important advance to obtain the spectra of nanocrystals one by one. We achieved this goal, recently, working with *ca.* 4 nm CdSe crystallites,

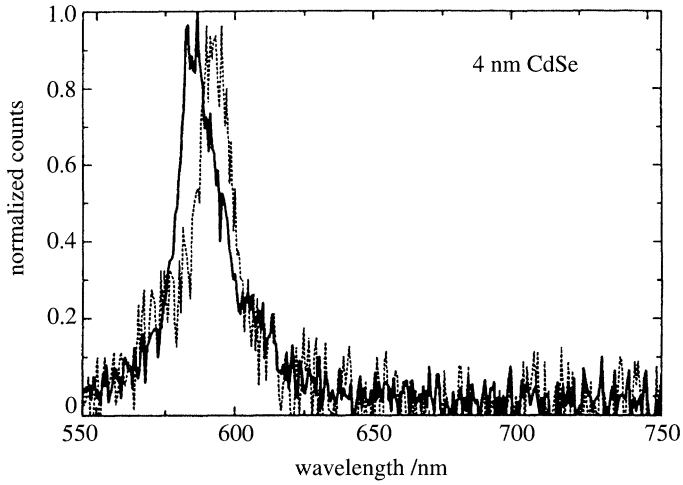

Figure 5. CdSe emission spectra of single nanocrystals.

using a room temperature NSOM apparatus (Betzig *et al.* 1991; Betzig & Trautman 1992; Trautman *et al.* 1994). Nanocrystals were spin-coated onto a transparent polymer surface at extreme dilution, such that, on average, several hundred nanometers separated neighbours. At this spatial resolution, the NSOM apparatus is able to record emission spectra one by one. The spectra presented in figure 5 are believed to originate from single crystallites. Distinct spectral shifts were observed from crystallite to crystallite, and the individual spectra were *ca.* 10 nm narrower than the far-field inhomogeneously broadened spectrum of many nanocrystals.

As with any new technique, near-field spectroscopy needed to be carefully characterised. In particular, we were concerned that the presence of the near-field probe would affect some of the optical properties of the sample. To better understand the possible perturbations, as well as to optimize the instrument, we have studied the near-field-excited, fluorescence emission of single molecules under ambient conditions (Trautman *et al.* 1994). In contrast to nanocrystals which have varying numbers of atoms, different surface bonding arrangements and the consequent variations in optical properties, molecules are all the same. Nevertheless, the spectrum of a collection of moelcules in a solution, on a surface or in a solid will be inhomogeneously broadened. The spectral distinctions are the result of variation in the coupling of the molecular excitation to the surroundings.

We studied 1,1′-dioctadecyl-3, 3′, 3′-tetramethylindocarbocyanine (diI) dispersed on polymethylmethacrylate (PMMA). DiI is well behaved on the polymer surface, exhibiting good photostability (many sequential excitation–emission cycles before photochemical bleaching) and an emission quantum yield near unity. It is possible to obtain good signal-to-noise emission spectra from approximately 50% of the molecules before photobleaching. Increasing the ratio to near unity could be achieved through improved detector technology or by decreasing the photobleaching probability. In general, the latter is less desirable as one would like to able to study single molecules in a variety of environments including in air, under water and at moderate (such as room) temperatures. The individual single-molecule spectra were observed to exhibit shifts of $+/-8$ nm relative to the average spectrum, and were typically narrower, as is expected for a far field, inhomogeneously broadened line. The spectra

PHILOSOPHICAL TRANSACTIONS OF THE ROYAL SOCIETY A MATHEMATICAL, PHYSICAL & ENGINEERING SCIENCES

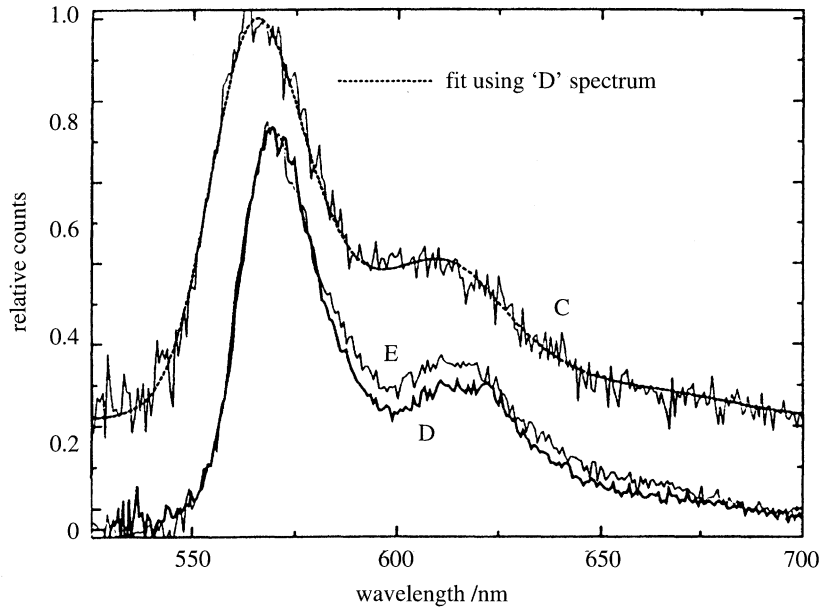

Figure 6. DiI single molecule emission specta, adapted from Trautman *et al.* (1994).

labelled 'D' and 'E' in figure 5 were among the narrowest obtained and exhibit a characteristic intensity difference in the vibronic band. The spectrum labelled 'C' is broadened, having a width comparable to that of the many-molecule spectrum. In addition, the emission spectra of approximately 20% of the individual molecules were found to exhibit time-dependent shifts of up to *ca.* 8 nm, from one minute to the next.

The variability in the spectral widths and the time-dependent shifts can be interpreted as consequences of dynamic modifications in the molecule's interaction with the local polymer polarizability. Those molecules having narrow spectra probably sit in relatively rigid environments, whereas those having broader spectra exist in more dynamic surroundings. In the latter case the molecular reorientation of the matrix molecules, and the concomitant shift in the emission wavelength, is supposed to occur many times within the one-minute spectral integration. Similarly, for the 'discrete' spectral jumps, the changes in the local environment occur on a time scale of minutes rather than seconds. Finally, we note that no correlation was found among the shift, the width, the time-dependence and the strength of the vibronic feature.

(*b*) *NSOM as an optical technology*

We have focused on the detection sensitivity of near-field optics because of the connection to the spectroscopy of semiconductor nanocrystals. Other capabilities of NSOM are, however, pertinent to nanotechnology as well. NSOM using the tapered, single-mode optical fibre probe (Betzig *et al.* 1991) is a versatile optical microscopy having resolution *ca.* $1/20\lambda$ in most imagining modes. The usual optical contrast mechanisms due to spatial variations in optical density, refractive index and birefringence are operative and frequently give rise to images similar to those observed in traditional far-field optics, excepting, of course, the improved resolution. In other cases, strong probe-sample coupling produces image contrast unique to NSOM. Ex-

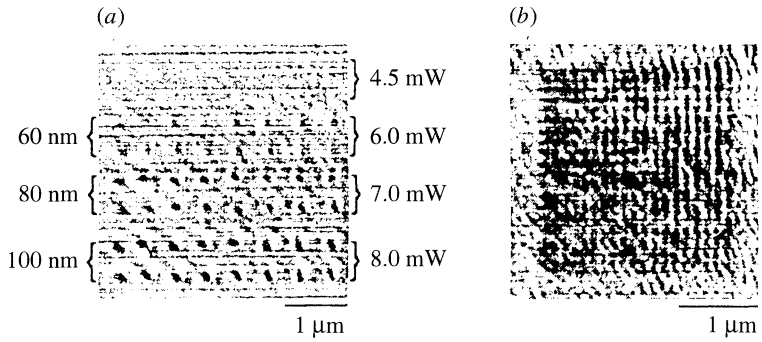

Figure 7. Near-field, Faraday-rotation images of magnetic domains written with an NSOM. (*a*) Image showing the effect of write power on the domain size. (*b*) A square, 20 × 20 array of domains on 120 nm centres, corresponding to a storage density of *ca.* 45 Gb in^{-2}. Adpated from Betzig *et al.* (1992).

amples of the latter may be found in Betzig & Trautman (1992). Here, we mention two cases exhibiting particularly strong near-field effects. These are, polarized light imaging near metallic edges, where the strigent boundary conditions imposed at a metal surface strongly affects the intensity of the light coupled out of the probe, and imaging of objects having only changes in refractive index, where the near-field contrast is dramatically enhanced relative to far-field imaging.

An active nanotechnology application of NSOM was demonstrated in experiments showing that the microscope could be used not only to produce Faraday rotation images of magnetic domains with *ca.* 30 nm resolution, but could also be used as a tool for writing magnetic bits down to *ca.* 60 nm diameter (Betzig *et al.* 1992), as shown in figure 7. To date, most near-field optical experiments have been designed to demonstrate the potential of the technique, rather than to either attack a particular scientific problem or to solve a specific technological need. The next few years should bring as much in the way of applications as the past few have brought in the way of potential.

References

Bawendi, M. G., Carroll, P. J., Wilson, W. L. & Brus, L. E. 1992 *J. Chem. Phys.* **96**, 946–1004.

Bawendi, M. G., Kortan, A. R., Steigerwald, M. L. & Brus, L. E. 1989 *J. Chem. Phys.* **91**, 7282–7290.

Bawendi, M. G., Wilson, W. L., Rothberg, L., Carroll, P. J., Jedju, T. M., Steigerwald, M. L. & Brus, L. E. 1990 *Phys. Rev. Lett.* **65**, 1623–1626.

Betzig, E. & Trautman, J. K. 1992 *Science* **257**, 189–195.

Betzig, E., Trautman, J. K., Harris, T. D., Weiner, J. S. & Kostelak, R. L. 1991 *Science* **251**, 1468–1470.

Betzig, E., Trautman, J. K., Wolfe, R., Gyorgy, E. M., Finn, P. L., Kryder, M. H. & Chang, C.-H. 1992 *Appl. Phys. Lett.* **61**, 142–144.

Brus, L. 1986 *J. Phys. Chem.* **90**, 2555–2560.

Brus, L. E. 1994 *J. Phys. Chem.* **98**, 3575–3581.

Brus, L. E., Szajowski, P. F., Wilson, W. L., Harris, T.D., Schnuppler, S. & Citrin, P. H. 1995 *J. Am. Chem. Soc.* **117**, 2915–2922.

Canham, L. T. 1990 *Appl. Phys. Lett.* **57**, 1046–1049.

Chestnoy, N., Hull, R. & Brus, L. 1986 *J. Chem. Phys.* **85**, 2237–2242.

PHILOSOPHICAL TRANSACTIONS OF THE ROYAL SOCIETY A MATHEMATICAL, PHYSICAL & ENGINEERING SCIENCES

Ekimov, A. I., Hache, F., Schanne-Klein, R. D., Flytzanis, C., Kudryatsev, I. A., Yazeva, T. V., Rodina, A. F. & Efros, Al. L. 1993 *J. Opt. Soc. Am.* B **10**, 100–107.

Lehmann, V. & Gosele, U. 1991 *Appl. Phys. Lett.* **58**, 856–859.

Littau, K.A., Szajowski, P. J., Muller, A. J., Kortan, A. R. & Brus, L. E. 1993 *J Phys. Chem.* **97**, 1224–1230.

Murray, C. B., Norris, D. J. & Bawendi, M. G. 1993 *J. Am. Chem. Soc.* **115**, 8076–8083.

Norris, D. J., Sacra, A., Murray, C. B. & Bawendi, M. G. 1994 *Phys. Rev. Lett.* **72**, 2612–2615.

Proot, J. P., Delerue, D. & Allan, G. 1992 *Appl. Phys. Lett.* **61**, 1948–1951.

Schoenlein, R. W., Mittleman, D. W., Shiang, J. J., Alivisatos, A. P. & Shank, C. V. 1993 *Phys. Rev. Lett.* **70**, 1014–1017.

Schuppler, S., *et al.* 1994 *Phys. Rev. Lett* **72**, 2648–2651.

Steigerwald, M. L., *et al.* al. 1988 *J. Am. Chem. Soc.* **110**, 3046–3050.

Takagahara, T. & Takeda, K. 1992 *Phys. Rev.* B **46**, 15 578–15 583.

Trautman, J. K., Macklin, J. J., Brus, L. E. & Betzig, E. 1994 *Nature* **369**, 40–42.

Wilson, W. L., Szajowski, P. F. & Brus, L. E. 1993 *Science* **262**, 1242–1244.

Xia, J. B. 1989 *Phys. Rev.* B **40**, 8500–8506.

PHILOSOPHICAL TRANSACTIONS OF THE ROYAL SOCIETY A MATHEMATICAL, PHYSICAL & ENGINEERING SCIENCES